Electronic Supplementary Information

Chemical engineering of *Mycobacterium tuberculosis* dodecin hybrids

Xenia Vinzenz, Wolfgang Grosse, Uwe Linne, Britta Meissner and Lars-Oliver Essen*

Philipps-Universität Marburg, Fachbereich Chemie, Hans-Meerwein-Strasse, 35032 Marburg, Germany.
E-mail: essen@chemie.uni-marburg.de; Fax: +49 6421 22032; Tel: +49 6421 22191

1. Experimental procedures

1.1 Construction of dodecin plasmids

The gene fragment coding for *Mycobacterium tuberculosis H37Rv* wild type dodecin (dodecin_wt) (YP_177647) coding for a 69 amino acid (aa) protein with a molecular mass of 7497.4 Da and a pI of 5.78 was amplified from the cosmid MTCY 277 with the 5' primer C GGG ATC CTC ATG AGC AAT CAC ACC TAC CG and the 3' primer G GGA ATT CTC GAG TTA TCA GGA ATC CTC CAG GCG (restriction sites for BspHI and XhoI underlined, respectively) and cloned into pET-28a(+) vector (*Novagen*) with the enzymes NcoI and XhoI.
Dodecin cysteine mutants were created on basis of this plasmid with the primers G AGC AAT CAC ACC TA**T** CGA **TGC** ATC GAG ATC GTC GGG ACC TCG and CGA GGT CCC GAC GAT CTC GAT GCA TCG ATA GGT GTG ATT GCT C for the V7C mutation (dodecin_C7), the primers GCG CTG GAC TGG TTC **TGC** GTA CA**A** TC**G** ATT CGA GGC CAC CTG and CAG GTG GCC TCG AAT CGA TTG TAC GCA GAA CCA GTC CAG CGC for the E40C mutation (dodecin_C40), the primers CTG GAC TGG TTC GAA GTA **TGT** TCA ATT CGA GGC CAC CTG G and C CAG GTG GCC TCG AAT TGA ACA TAC TTC GAA CCA GTC CAG for the Q42C mutation (dodecin_C42) as well as the primers GCG CAC TTC CAG GTG **TG**T ATG AAA GTC GGC TTC CG and CG GAA GCC GAC TTT CAT ACA CAC CTG GAA GTG CGC for the T59C mutation (dodecin_C59), analytical restriction sites for the enzyme ClaI (dodecin_C7, dodecin_C40) are underlined and mutations given in bold letters. All constructs were verified by sequence analysis (*Qiagen*).

1.2 Expression and purification of dodecin wildtype and cysteine mutants

Expression of *M. tuberculosis* dodecin_wt and its cysteine mutants was performed in *E. coli* BL21-Gold (DE3) cells (*Invitrogen*) transformed with the corresponding plasmids. Cells were grown in TB medium containing 35 μg/mL kanamycin for 24 hours to promote autoinduction at 37 °C for dodecin_wt, dodecin_C7 and dodecin_C59. In case of dodecin_C40 and dodecin_C42 cells were grown at 37 °C to an optical density at 595 nm of 0.5, afterwards cooled to 18 °C and further incubated at this temperature. Expression cultures were harvested (6400 *g*, 20 min, 4 °C), resuspended in AM buffer I (20 mM Tris/HCl pH 8.0, 200 mM NaCl) in case

of dodecin_wt or AM buffer II (10 mM Tris/HCl pH 8.0, 100 mM NaCl) in case of cysteine mutants and shock frozen in liquid nitrogen.

Cells were broken using the Emulsiflex C5 (*Avestin*) and crude cell extract was centrifuged (25402 *g*, 20 min, 4 °C). As a highly efficient purification step the thermostability of dodecin was utilized, which shows no denaturation in circular dichroism spectroscopy upon being heated to 95 °C for 60 min (data not shown). The supernatant was hence heated in a water bath at 70 °C for 10 min for dodecin_wt and at 85 °C for 30 min in case of dodecin cysteine mutants, then centrifuged (3220 *g*, 25 min, 4 °C), applied to an ion-exchange column (Q Sepharose, *GE Healthcare*) under buffer A (20 mM Tris/HCl pH 8.0) and washed with 4 CV. Elution was performed with a linear gradient over 4 to 6 CV of 0 - 100% buffer B (20 mM Tris/HCl pH 8.0, 1 M NaCl) and the column was afterwards washed with 4 CV. Fractions were pooled and concentrated to 20 mg/mL using an Amicon® Ultra membrane (*Millipore*) with a MWCO of 10000 Da.

All samples except of the FMN-free dodecin samples were reconstituted over night at 20 °C in the dark with a 15% molar excess of FMN after S-alkylation or depletion of cofactor. Afterwards a size exclusion chromatography (Superdex 200, *GE Healthcare*) was carried out with SEC buffer (20 mM Tris/HCl pH 8.0, 100 mM NaCl) and the main peak was pooled and concentrated to 20 mg/mL.

1.3 Synthesis of dansyl modulator

N-(2-Ethyl-iodo-acetamide)-dansyl (dansyl) was prepared as described by Reitz *et al.*[1] and stored at -80 °C until usage.

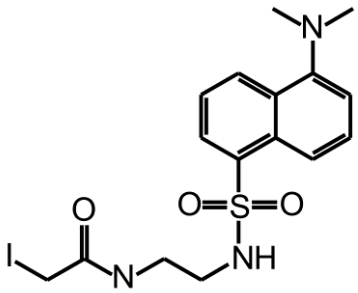

Fig. S1 Structure formula of N-(2-Ethyl-iodo-acetamide)-dansyl (dansyl) as used for modification of dodecin.

1.4 S-alkylation in folded state and denatured state

For the modification of dodecin in the folded, dodecameric state different reaction times, buffers, protein purification grades and the addition of 1 mM TCEP were tested. Optimal results were obtained, when dodecins purified *via* IEX were transferred to alkylation buffer N (0.1 M potassium phosphate, pH 7.5) at a concentration of 10 mg/mL, dansyl (100 mM in MeCN) was added to a final concentration of 3 mM and incubated for 19 h at 37 °C under gentle shaking. The reaction was stopped by addition of 50 mM DTT at room temperature and incubation for 10 min.

For the coupling reaction in the denatured state a likewise screening in buffers containing urea or guanidinium chloride (GdnCl) resulted in the same conditions using alkylation buffer U (0.1 M potassium phosphate, pH 7.5, 6 M urea).

The success of the reaction was monitored by SDS-PAGE under UV-light (λ_{max} = 325 nm) and documented with a camera (*Nikon* D60) using a UV-filter (BP-590 50, *Schneider*). Excess dansyl was removed by a PD-10

desalting column (*GE Healthcare*). In case of denatured dodecin samples protein was refolded in presence of FMN (ESI 1.5) or in case of folded dodecin reconstituted with FMN and further purified by SEC as described in ESI 1.2.

1.5 Refolding of dodecin

To obtain cofactor-free dodecin the samples purified *via* IEX were strongly diluted with L1 buffer (20 mM Tris/HCl pH 8.0, 100 mM NaCl, 6 M GdnCl) to a final concentration of 1 mg/mL. Addition of 7.2% TCA and heating in a water bath for 15 min at 65 °C resulted in precipitation of protein without cofactor. After centrifugation (25402 *g*, 30 min, 4 °C) dodecin was obtained as white pellet, which was solved in L1 buffer at a concentration of 1 mg/mL.

Denatured dodecin in L1 buffer or alkylation buffer U (ESI 1.4) was dialyzed (3.5 MWCO SnakeSkin®, *Thermo*) in five steps over one week against SEC buffer to a final concentration of denaturing agent of less than 20 mM. Pure refolded dodecin was then applied to SEC as described in ESI 1.2.

1.6 Spectroscopic measurements

Absorption spectra in solution for dodecin, its hybrids and free compounds were recorded with an Ultrospec 3100pro UV/Visible Spectrophotometer (*GE Healthcare*), SWIFT II software (*Biochrom Ltd.*) using a SUPRASIL 200 µL cuvette (Type 105.200-QS, *Hellma*) at room temperature. Samples were diluted to obtain a maximum signal of 2 OD units and scanned with 250 nm/min. Absorption measurements of dodecin and hybrid crystals were performed at the ESRF cryobench (Grenoble) using a type HR2000+ spectrometer and a DH-2000-BAL (*Ocean Optics*) light-source. Spectra were recorded using air as reference, an integration time of 70 ms, averaging of 10 spectra and without boxcar smoothing.

Fluorescence emission spectroscopy in solution was performed using a FP-6500 spectrofluorometer (*Jasco*) with a SUPRASIL 10 mm light path cuvette (*Hellma*) at 20 °C. Samples were excited at a wavelength of 355 nm (band widths for excitation 5 nm, emission 5 nm) in steps of 1 nm, 500 nm/s scanning speed, medium sensitivity, 0.5 s response time and accumulation of 3 spectra. Emission spectra of dodecin and hybrid crystals were measured at the cryobench with the above mentioned setup and a wavelength of 355 nm for excitation.

Fluorescence excitation spectroscopy was performed using the FP-6500 spectrofluorometer with the same specifications as for the emission spectroscopy monitoring the fluorescence intensity at the emission wavelength of 528 nm. All spectra in solution were measured in SEC buffer.

1.7 Mass spectrometry

For mass spectrometric analysis 0.25 µg protein in SEC buffer at a concentration of 10 - 20 mg/mL was used. For complete desalting of the proteins using an Agilent 1100 HPLC system, samples were applied to a monolithic 50/1 ProSwift RP-4H column (*Dionex*). Desalted proteins were eluted by a gradient of buffer A (water/0.05% formic acid) to buffer B (acetonitrile/0.045% formic acid) at a column temperature of 40°C and a flow rate of 0.2 mL/min with an isocratic elution with 5% A for two minutes, followed by a linear gradient to 95% B within 8 min and holding 95% B for additional 4 min.

Online mass spectrometric analysis was carried out with a Qstar Pulsar i mass spectrometer (*ABSciex*) equipped with an ESI source. Parameters were DP1 75, FP 265, DP2 15, CAD 2, GS1 65, CUR 35. The voltage applied was 5500 V. Positive ions within the mass range of 500-2000 m/z were detected. For better performance, the "Enhance All" mode was activated.

Theoretical average masses of protonated compounds were calculated using the *Peptide Mass Calculator v3.2* online tool from *Katholieke Universiteit Leuven* (http://rna.rega.kuleuven.ac.be/masspec/pepcalc.htm).

1.8 Crystallization of wild type dodecin and hybrids

Yellow-colored crystals of *M. tuberculosis* dodecin_wt were grown using the hanging drop vapor diffusion technique at 20 °C and SEC-purified protein at a concentration of 9 mg/mL protein and a two-fold molar excess of CoA in SEC buffer. 1 µL of protein solution was mixed with 1 µL of reservoir solution (10 mM $CoCl_2$, 100 mM NaOAc pH 5.0, 200 mM hexanediol) and equilibrated against 1 mL reservoir solution. Large, cubic shaped crystals appeared within a few days and were flash frozen in liquid nitrogen after addition of 20% glycerol as cryo-protectant.

For the crystallization of dodecin hybrids the SEC-purified proteins were incubated over night with a 3-fold molar excess of CoA at 20 °C and used in concentrations of 10 mg/mL to 20 mg/mL with commercially available screening kits (*Qiagen*) in 96-well crystallization plates (*Innovadyne*). Here, the sitting drop vapor diffusion technique was applied by mixing 300 nL of protein solution with 300 nL of reservoir solution and equilibration against 80 µL of reservoir. Yellow-colored crystals grew within four to six weeks in various conditions yielding the best diffracting ones for the dodecin_C59-dansyl hybrid from condition 85, $(NH_3)_2SO_4$ suite (*Qiagen*, 2 M NaCl, 2 M $(NH_3)_2SO_4$) with 10 mg/mL protein. Crystals could be directly flash frozen in liquid nitrogen due to the high salt concentration.

1.9 Data collection, structure solution and refinement

Diffraction data with a maximum resolution of 1.7 Å for the dodecin_wt were collected at beamline BW7A at the EMBL outstation Hamburg using a wavelength of 0.9184 Å and a temperature of 100 K. Data were processed by MOSFLM[2] and scaled with the program SCALA (CCP4i package[3]) in space group H32 (a = b = 94.30 Å, c = 230.91 Å, $\alpha = \beta = 90°$, $\gamma = 120°$) with four molecules per asymmetric unit. The structure was solved using MOLREP[4] with the *T. thermophilus* dodecin (pdb code 2V21)[5] as search model. REFMAC5[6] was used for refinement and COOT[7, 8] was used for manual model building.

For the dodecin_C59-dansyl 300 images of diffraction data with 0.5° per image and a resolution of 2.1 Å were collected at beamline ID23-2 at the ESRF, Grenoble, at a temperature of 100 K and a wavelength of 0.87260 Å. Data were indexed and scaled by XDS and XSCALE[9, 10] in space group $C222_1$ (a = 94.16 Å, b = 104.01 Å, c = 82.64 Å; $\alpha = \beta = \gamma = 90°$) at a resolution of 2.4 Å. Structure solution was performed by molecular replacement using the program PHASER[11] (CCP4i package) with six molecules per asymmetric unit, i. e. half a dodecin dodecamer, and the dodecin_wt structure as search model. Refinement was performed using REFMAC5 (CCP4i package) and COOT for manual model building. Restraints for the dansyl compound were the same as described by Grosse *et al.*[12]

1.10 Estimation of maximum size of incorporated compounds

To estimate the inner volume of dodecin_wt, which cannot be treated as an ideal sphere, the program HOLLOW[13] version 1.1 was used with a grid spacing of 0.7 Å and an interior probe radius of 1.444 Å to create dummy atoms filling the inner cavity. The volume of the atoms in the sphere was calculated using UCSF Chimera[14] resulting in a value of 9649 $Å^3$.

Assuming a protein-like atomic composition, compounds filling the cavity will occupy a volume of ~0.74 cm^3/g or 0.813 $Da/Å^3$.[15] Using the total volume of 9649 $Å^3$, or 804 $Å^3$ per monomer, compounds introduced into the inner cavity may have a size of up to 0.65 kDa without additional water. Accordingly, assuming a realistic water content of 50%, ca. 0.33 kDa may be introduced per monomer for any artificial compound. This fits well with the assumption that the additional 334 Da provided by covalent modification with dansyl are close to the upper capacity limit of space in the sphere.

2. Supplementary results

2.1 Analysis of different dodecin hybrids

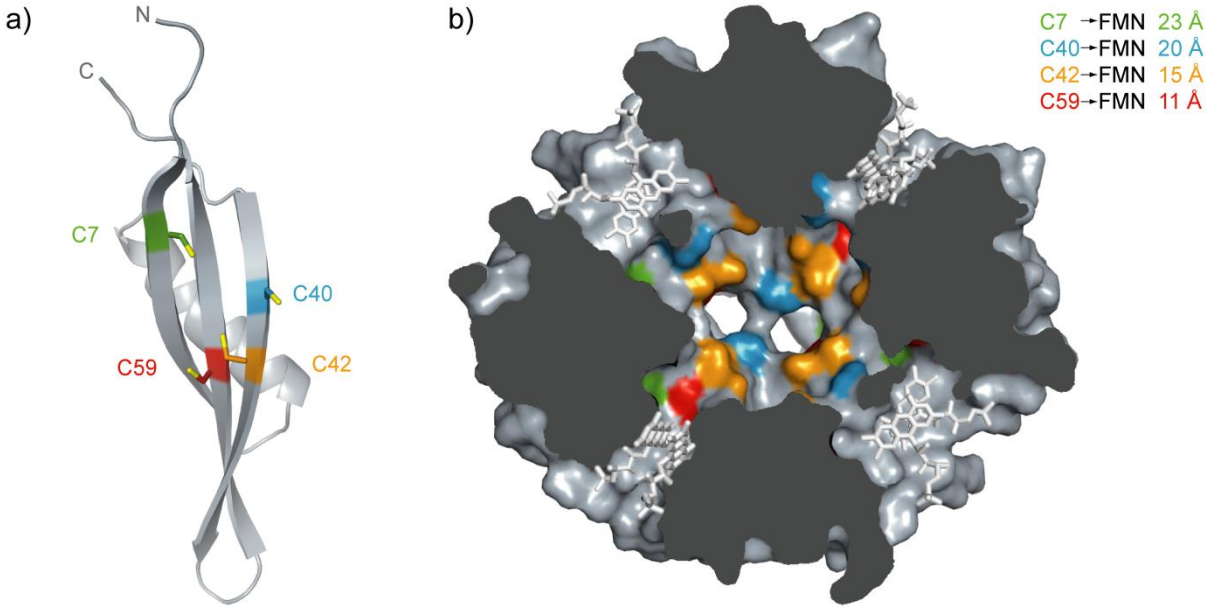

Fig. S2 Location of different cysteine mutations shown for a representative dodecin monomer (a) and their positions in the dodecameric sphere where they point inwards as depicted by the sectional view showing half a dodecamer (b).

The success of the S-alkylation reaction was determined by mass spectrometry and SDS-PAGE as described in ESI 1.7 and ESI 1.4, respectively, using the intrinsic fluorescence of dansyl. Fig. S3 and Fig. S4 show dodecin-dansyl hybrids prepared by reaction under native conditions of all four mutants before and after removal of excess dansyl as well as dodecin_wt serving as reference. Interestingly, only dodecin_C59-dansyl is still apparent in the dodecameric state in a denaturing PAGE as usually observed for dodecin_wt (Fig. S4). All other mutants disassemble to their monomeric state under the denaturing conditions chosen for SDS-PAGE. To examine correct folding of the mutants a native PAGE was performed showing that all dodecin-hybrids and dodecin_wt assemble to intact dodecamers when not being denatured. Dodecin_wt shows residual fluorescence after PD-10 desalting column, which corresponds to some unspecific binding of dansyl to the cysteine-free wild

type. Analogous to the dodecin_C59-dansyl the dansyl moiety may be here unspecifically bound in the FMN binding pocket.

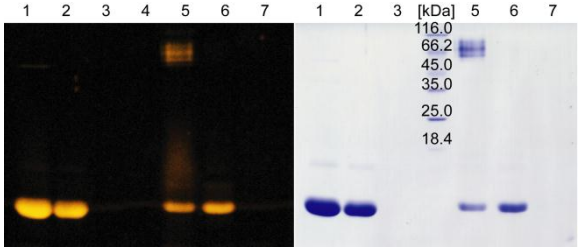

Fig. S3 15% SDS-PAGE under denaturing conditions of dodecin dansyl hybrids under UV-light (λ_{max} = 325 nm) (left) and Coomassie stained (right): dodecin_C7 after 19 h incubation with dansyl (lane 1), mixture after PD-10 desalting column (lane 2), flow through of concentrator (lane 3), molecular weight marker (lane 4), dodecin_C40 after 19 h incubation with dansyl (lane 5), mixture after PD-10 desalting column (lane 6), flow through of concentrator (lane 7).

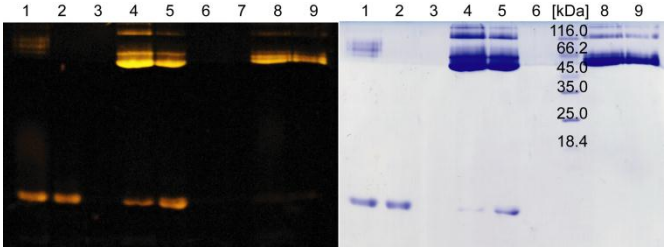

Fig. S4 15% SDS-PAGE under denaturing conditions of dodecin dansyl hybrids under UV-light (λ_{max} = 325 nm) (left) and Coomassie stained (right): dodecin_C42 after 19 h incubation with dansyl (lane 1), mixture after PD-10 desalting column (lane 2), flow through of concentrator (lane 3), dodecin_C59 after 19 h incubation with dansyl (lane 4), mixture after PD-10 desalting column (lane 5), flow through of concentrator (lane 6), molecular weight marker (lane 7), dodecin_wt after 19 h incubation with dansyl (lane 8), mixture after PD-10 desalting column (lane 9).

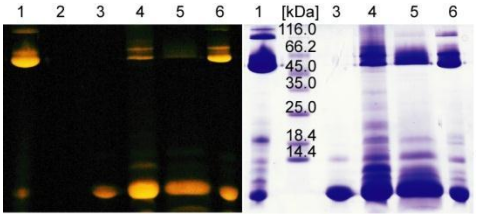

Fig. S5 15% SDS-PAGE under denaturing conditions of dodecin dansyl hybrids produced in unfolded state by incubation over night with dansyl and refolding in presence of FMN subsequently under UV-light (λ_{max} = 325 nm) (left) and Coomassie stained (right): dodecin_wt (lane 1), molecular weight marker (lane 2), dodecin_C7-dansyl (lane 3), dodecin_C40-dansyl (lane 4), dodecin_C42-dansyl (lane 5) and dodecin_C59-dansyl (lane 6).

For the dodecin hybrids the refolding yields were worse than for dodecin_wt (wt: 85%, C7: 3%, C40: 15%, C42: 20%, C59: 80%). Therefore refolding of dodecin variants without FMN, in presence of FMN and after reaction with iodoacetamide (*Sigma Aldrich*) or dansyl (ESI 1.4) was carried out as described in ESI 1.5. After adding 2 mM FMN to the sample, refolding yields generally increased by 30%-90%. The cysteine comprising dodecin variants have diminished refolding yields, which were site-dependent, resulting in losses between 5 and 80%. Inactivation of the reactive thiol side-chains with the sterically less demanding iodoacetamide or the more demanding dansyl resulted again in site-dependent, but size-independent yields. For the relatively small iodoacetamide no improvement was observed, whereas the introduction of dansyl gave decreased refolding yields only for dodecin_7C, but increased yields for the other tree cysteine mutants.

2.2 Spectroscopic analysis of dodecins and hybrids

Spectroscopic analysis of *M. tuberculosis* dodecin_wt and its hybrids was performed with absorption, fluorescence emission and fluorescence excitation spectroscopy as described in ESI 1.6.

Fig. S6a shows the typical maxima for FMN at 266 nm, 372 nm and 446 nm and for dansyl at 247 nm and 330 nm. The double peak (372 nm, 446 nm) from FMN is clearly discernible in the FMN-reconstituted dodecin_wt and dodecin_C59, but not in the FMN-depleted dodecin. The 266 nm peak shows a shift to 272 nm in the bound form. In comparison the dansyl hybrids show a strong shift of this peak from 272 nm to shorter wavelengths at 260 nm ± 1 nm, which very likely results from an overlap of the dansyl peak at 247 nm and the FMN peak at 266 nm/272 nm. At the same time the FMN double peak (372 nm, 446 nm) is less pronounced in all hybrids (Fig. S6b). Dodecin_C59-dansyl shows a different behavior than the other mutants where no distinct peaks in the range between 300 nm and 500 nm are visible. *In crystallo* absorption spectra of the crystals obtained for two of the dansyl hybrids show a variance in the 372 nm maximum of the FMN double peak in comparison to dodecin_wt crystals (Fig. S6b). Depending on the mutant the 372 nm peak is more (dodecin_C59-dansyl) or less (dodecin_C7-dansyl) strongly shifted towards shorter wavelengths. This can be explained with an overlap with the 330 nm maximum of dansyl, whereas a statement for the more significant peak in solution spectra at 260 nm cannot be made due to the strong absorption of dodecin crystals.

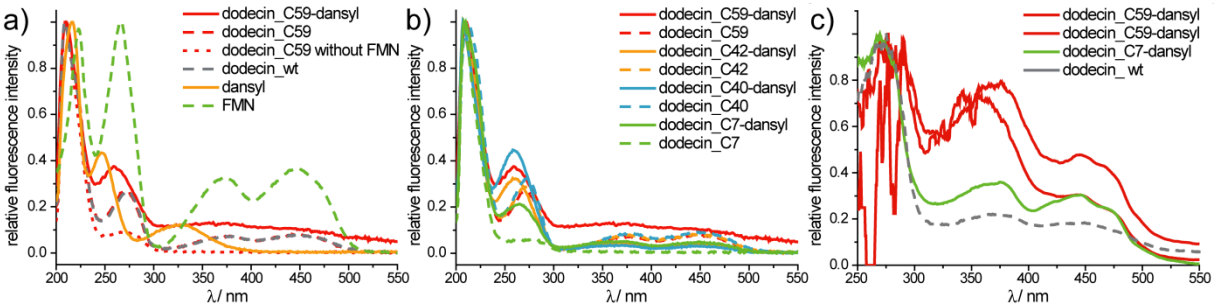

Fig. S6 Absorption spectra of dodecin_wt and dodecin hybrids. (a) Normalized spectra in SEC buffer at room temperature of dodecin_wt, dodecin_C59 with and without FMN, dodecin_C59-dansyl, dansyl and FMN as references. (b) Comparison of all four dodecin cysteine mutants and their corresponding dansyl hybrids in SEC buffer at room temperature. (c) *In crystallo* absorption spectra (smoothed by 10 point adjacent averaging) of dodecin_wt, dodecin_C7-dansyl and dodecin_C59-dansyl of different crystals measured at 100 K.

In fluorescence emission spectroscopy signals in solution for dansyl (547 nm) and FMN (528 nm) at an excitation wavelength of 355 nm are relatively close (Fig. S7a). For dodecin and its cysteine mutants reconstituted with FMN the spectrum mainly consists of the strong FMN signal at 528 nm. Dodecin dansyl hybrids show no significant difference in spectra, but a fronting can be observed for the corresponding signals (Fig. S7b). The strongest fronting can be observed for dodecin_C59-dansyl, which strongly differs from other hybrids, even resulting in a shift of the maximum from 528 nm to 522 nm. Spectra from crystals show a strong difference between hybrids and the dodecin_wt. The signal of FMN is quenched in the *in crystallo* measurements,[16] giving no significant signal for dodecin_wt (Fig. S7c). The signal for dansyl is not quenched, so that maxima appear strongly shifted to shorter wavelength at ~514 nm and the characterized mutants dodecin_C7-dansyl and dodecin_C59-dansyl show similar behavior. Fronting observed in solution due to overlay with the FMN signal corresponds here with a stronger shift of the maximum to shorter wavelength as FMN is not detected.

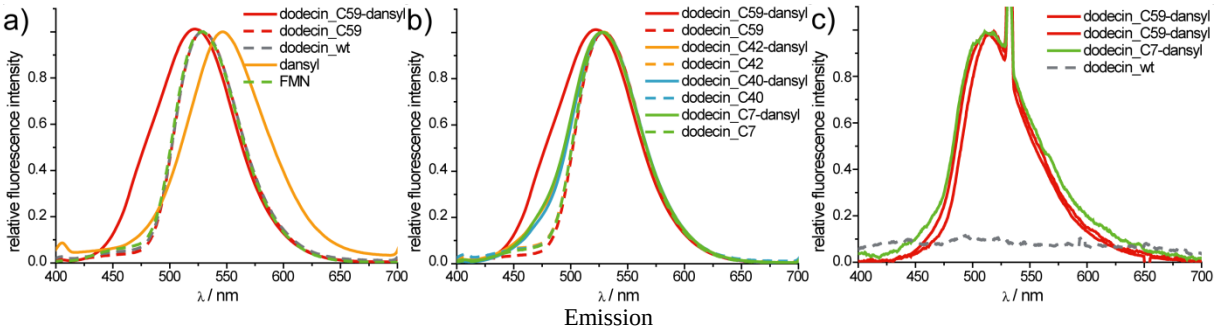

Fig. S7 Fluorescence emission spectra of dodecin_wt and dodecin hybrids. All spectra were measured with an excitation wavelength of 355 nm and normed on their maximum between 500 nm and 550 nm. (a) Spectra in SEC buffer at 293.2 K of dodecin_wt, dodecin_C59 with FMN, dodecin_C59-dansyl hybrid unsing dansyl and FMN as references. (b) Comparison of all four dodecin cysteine mutants and their corresponding dansyl hybrids in SEC buffer at 293.15 K. (c) *In crystallo* absorption spectra (smoothed by 10 point adjacent averaging) of dodecin_wt, dodecin_C7-dansyl and dodecin_C59-dansyl of different crystals measured at 100 K.

Fluorescence excitation spectroscopy gives the most distinct signals for FMN and dansyl at an emission wavelength of 528 nm with a double peak for FMN at 373 nm and 450 nm and a single signal for dansyl at 330 nm. All spectra were measured in solution and normed to the 450 nm FMN maximum. As observed by emission fluorescence spectroscopy all FMN-reconstituted dodecin variants as well as dodecin_wt give similar spectra. (Fig. S8) dominated completely by FMN. For dodecin dansyl-hybrids a strong increase in signal intensity and a strong shift to shorter wavelengths of the 373 nm peak is visible. Outstanding is the shift observed for dodecin_C59-dansyl of 73 nm as well as the significantly increased signal, which both might be a result of dansyl occupying the FMN binding pocket and therefore a lower FMN concentration in the sample. The other mutants show a less significant shift of 12 nm for dodecin_C7-dansyl, 8 nm for dodecin_C49-dansyl and 7 nm for dodecin_C40-dansyl. To get spectra dominated by the dansyl modification, spectra of unmodified dodecin cysteine mutants were subtracted of the according dansyl hybrid (Fig. S8c). Here a shift of 10 ±1 nm for the covalently bound dansyl in a changed chemical environment can be observed for the hybrids.

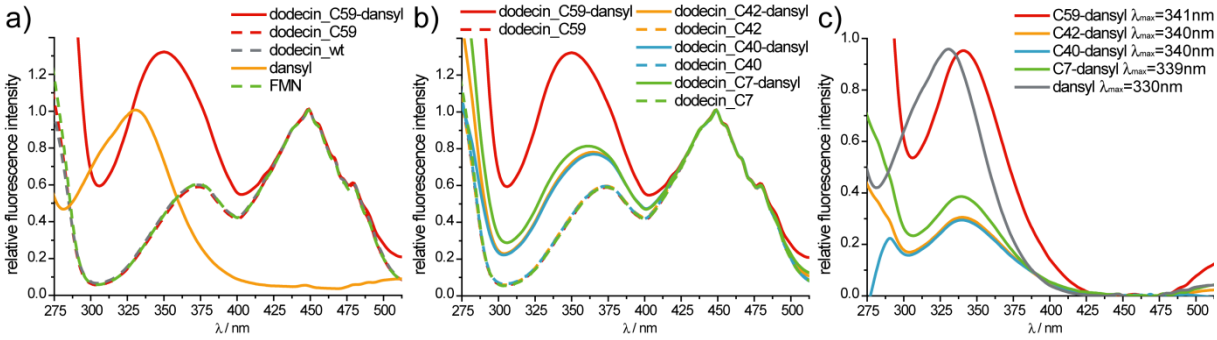

Fig. S8 Fluorescence excitation spectra of dodecin_wt and dodecin hybrids. All spectra were measured with an emission wavelength of 528 nm and normed on their maximum at 450 nm. (a) Spectra in SEC buffer at 293.2 K of dodecin_wt, dodecin_C59 with FMN, dodecin_C59-dansyl hybrid using dansyl and FMN as references. (b) Comparison of all four dodecin cysteine mutants and their corresponding dansyl hybrids in SEC buffer at 293.15 K. (c) Difference spectra of the dodecin dansyl hybrids minus their corresponding FMN-reconstituted spectra, pure dansyl is given as a reference.

Due to the differences observed in fluorescence spectroscopy the amount of FMN bound to the dodecin-dansyl hybrids was compared to dodecin_wt. The absorption of FMN at 450 nm is mostly independent of all other components, allowing to derive FMN-contents from spectral information. The 280 nm peak is not representing protein only, but a sum of the apoprotein, FMN and the covalent dansyl modification. Assuming a quantitative reaction, the absorption coefficient for the protein-dansyl hybrid can be calculated, reducing the concentration

dependent variables to one. After subtraction of the calculated FMN contribution of the 280 nm absorption, the protein concentration can be derived. For calculation molar extinction coefficients from Oregon Medical Laser Center (OMLC) for riboflavin[17] and dansyl-glycine[17] were used, the latter exactly matching our experimental data for the dansyl-compound. For the calculation of the molar extinction coefficient of the apoprotein the ProtParam tool[18] on www.expasy.org was used. The corresponding values applied in calculations were ε_{280}(dodecin) = 6990 $M^{-1}cm^{-1}$; ε_{280}(dansyl) = 1596 $M^{-1}cm^{-1}$; ε_{280}(FMN) = 18167 $M^{-1}cm^{-1}$ and ε_{280}(FMN) = 10677 $M^{-1}cm^{-1}$.

The absorption values at 280 nm and 450 nm were determined during SEC, where only FMN directly bound to dodecin elutes at the same time. All dodecin dansyl hybrids seem to incorporate less FMN than dodecin_wt. As with the absorption spectra, dodecin_C59-dansyl shows the lowest amount of FMN bound, supporting our findings of dansyl covalently attached within reach of the FMN-binding pocket. The observed c(FMN)/c(protein) ratios were 0.49 for dodecin_wt, 0.38 for dodecin_C7-dansyl, 0.23 for dodecin_C40-dansyl, 0.47 for dodecin_C42-dansyl and 0.14 for dodecin_C59-dansyl. The obtained value for dodecin_wt is below the expected 1:1 stoichiometry as described for the *Thermus* dodecin[5]. Besides putative systematic errors in the calculation using hypothetical extinction coefficients, the obtained values are sufficient for estimating a loss in FMN-binding. Unlike *Thermus* dodecin, we found that FMN is less stably bound to the *M. tuberculosis* dodecin, because it can be generally removed by dialysis.

2.3 Mass spectrometry

All hybrids, mutants and wild type dodecin were verified by mass spectrometry as described in ESI 1.7 and gave positive results. Exemplifying for the unmodified proteins dodecin_wt and dodecin_C59-dansyl are shown in Fig. S9. All four dodecin dansyl hybrids are depicted in Fig. S10.

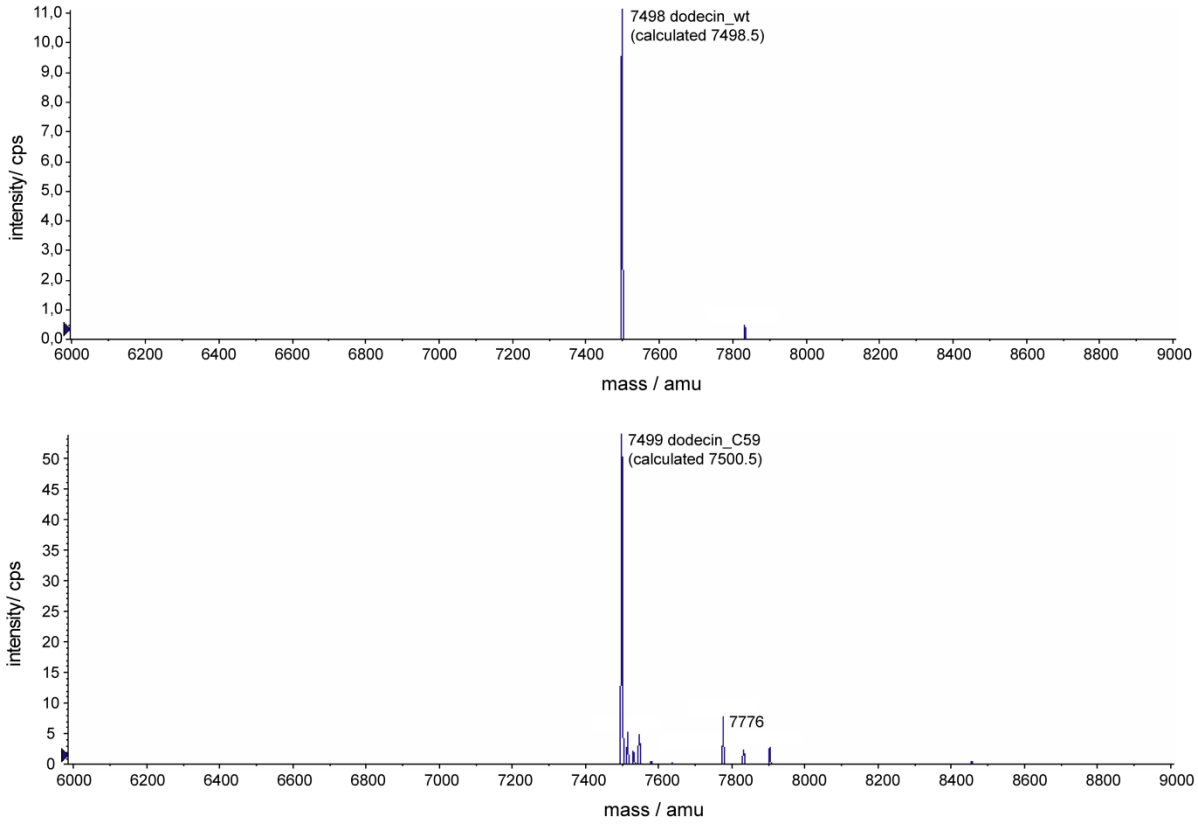

Fig. S9 Mass spectrometric analysis of dodecin_wt (top) and dodecin_C59 (down) with corresponding signals and calculated masses.

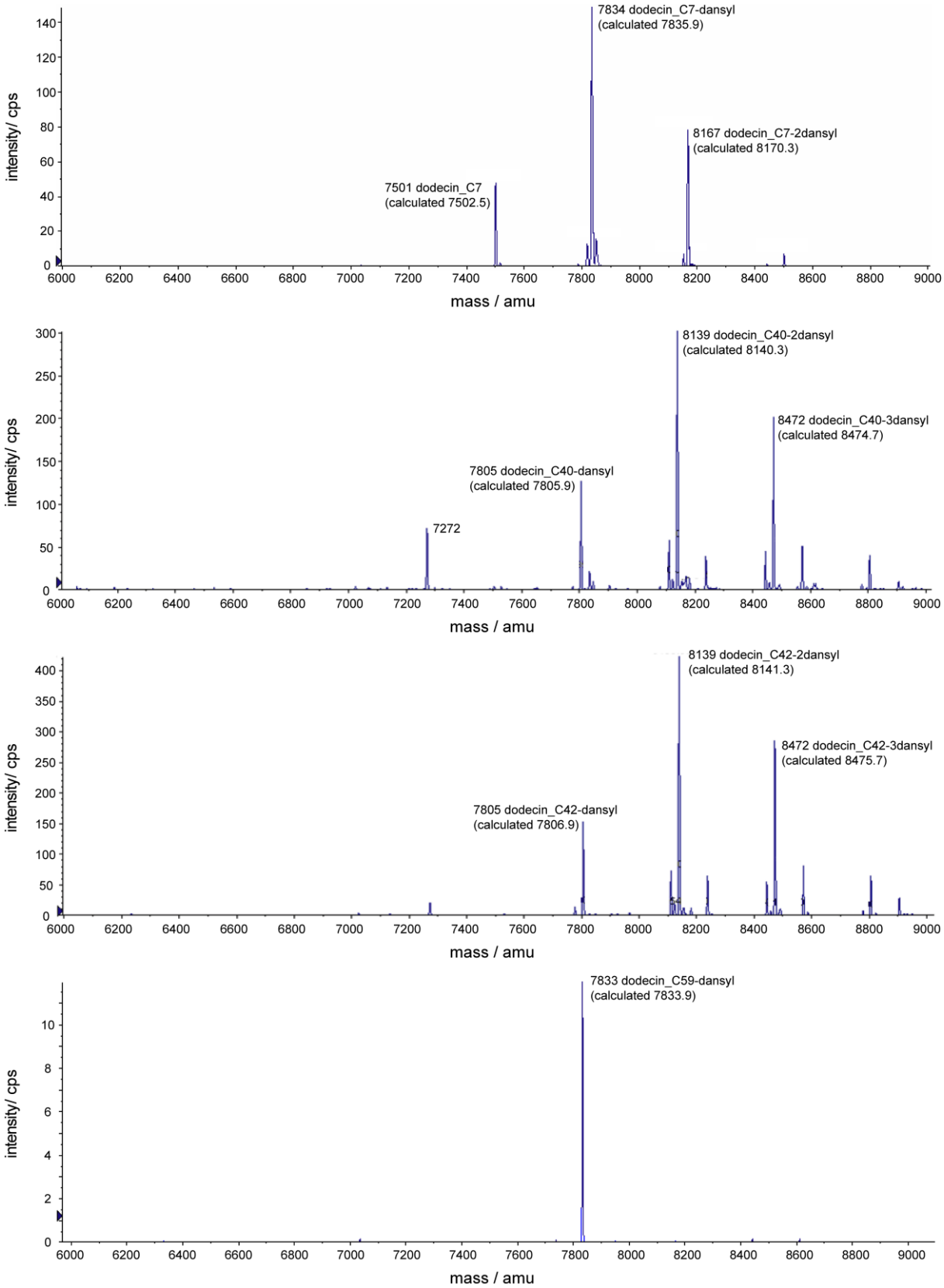

Fig. S10 Mass spectrometric analysis of dodecin_C7-dansyl, dodecin_C40-dansyl, dodecin_C42-dansyl and dodecin_C59-dansyl (top to bottom) with corresponding signals and calculated masses.

2.4 Crystallographic table

Table S1 Crystallographic table of dodecin_wt and dodecin_C59-dansyl.

Data collection and processing	**dodecin_C59-dansyl** **2YJ0**	**dodecin_wt** **2YIZ**
X-ray source	ID23-2, *ESRF*	BW7A, *DESY*
Wavelength [Å]	0.87260	0.91840
Detector	MARMOSAIC 225 CCD	MAR CCD M300
Temperature [K]	100	100
Space group	$C222_1$	H32
molecules per asymmetric unit	6	4
Cell dimensions		
a, *b*, *c* [Å]	94.00, 103.80, 82.50	94.30, 94.30, 230.91
α, β, γ, [°]	90.00, 90.00, 90.00	90.00, 90.00, 120.00
Resolution [Å][a]	47.08-2.40 (2.53-2.40)	14.91-1.70 (1.79-1.70)
Observed reflections	99276	486357
Unique reflections	16225	43832
Multiplicity[a]	6.1 (6.2)	11.1 (11.1)
R_{merge}[a, b]	0.108 (0.689)	0.052 (0.775)
Completeness [%][a]	99.9 (100.0)	99.9 (100.0)
$\langle I \rangle / \sigma \langle I \rangle$[a]	15.2 (2.8)	24.8 (3.3)
Mosaicity [°]	0.17	0.30
Wilson *B*-factor [$Å^2$]	39.9	26.7
solvent content	0.431	0.614
Refinement statistics		
Resolution [Å][a]	25.00-2.40 (2.46-2.40)	14.91-1.70 (1.74-1.70)
R_{work} , R_{free} [%][a, c, d]	21.7, 27.5 (28.1, 38.5)	17.2, 19.7 (19.6, 22.1)
Reflections (working set, test set)[a, d]	15214, 974 (1101, 65)	42659, 1084 (3104, 73)
Rmsd bond lengths from ideal [Å]	0.005	0.012
Rmsd bond angles from ideal [°]	1.156	1.342
Number of atoms (total; protein, hetero, water)	4007; 3357, 487, 163	2670; 2181, 228, 261
Mean *B* value (total; protein, hetero, water) [$Å^2$][e]	21.8 (27.6); 27.5, 26.9, 33.7	28.0 (37.9); 35,9, 43.9, 49.3

a Values in parentheses correspond to the highest resolution shell.

b $R_{merge} = \sum_{hkl} \sum_i \left| I_i(hkl) - \langle I(hkl) \rangle \right| \div \sum_{hkl} \sum_i I_i(hkl)$.

c $R_{work} = \sum \left| F_{obs} - F_{calc} \right| \div \sum (F_{obs})$.

d R_{free} crystallographic R-factor based on 6% (dodecin_C59-dansyl) or 2.5% (dodecin_wt) of the data withheld from the refinement for cross-validation.

e Values in parenthesis correspond to mean *B* values obtained without TLS refinement.

2.5 CoA-binding pocket of *M. tuberculosis* dodecin

The strong crystallization tendency of the highly symmetric dodecin complexes allowed obtaining crystals in several conditions exhibiting different space groups. Crystallographic data for the above mentioned structure for dodecin_wt gave only averaged and fragmented electron density for the CoA cofactor, because in this crystal form (space group H32) the trimeric interface II[5] corresponds to the crystallographic 3-fold axis. In contrast, the dodecin_C59-dansyl crystal obtained in space group $C222_1$ showed continuous electron density for a unique conformation of CoA, as here only local, non-crystallographic symmetry prevails.

As observed for the *T. thermophilus* dodecin (pdb-accession code: 2V18) CoA is bound as a trimer in a V-shaped conformation. The only significant difference in binding is given by the orientation of two phosphate groups (Fig. S11a). Electron density for the CoA molecule showing proper definition in the dodecin_C59-dansyl structure is given in Fig. S11b.

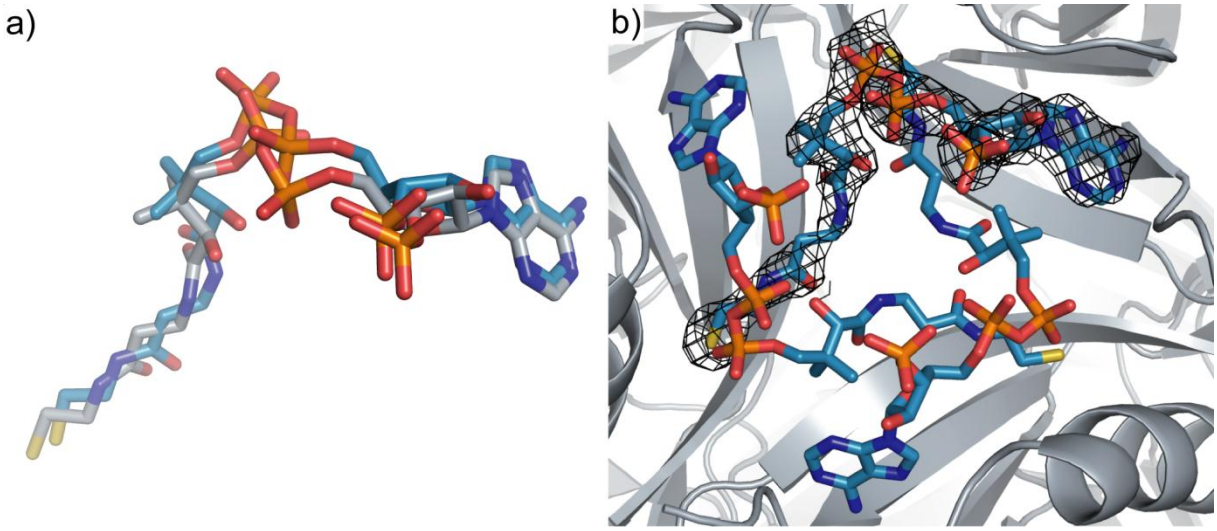

Fig. S11 Stoichiometric binding of CoA cofactor to dodecin in V-shaped conformation. (a) Comparison of CoA binding in *T. thermophilus* (grey) and *M. tuberculosis* hybrid (blue). (b) SIGMAA-weighted electron density (dark grey) for one of the three CoA molecules (blue) bound to trimeric interface II[5] as observed in the dodecin_C59-dansyl structure (grey) at a contouring level of 1.25 $\sigma \equiv 0.43$ e/Å^3.

2.6 Comparison of dodecin hybrid and wild type structure

The dodecin_C59-dansyl hybrid showed strong differences compared to dodecin_wt in spectroscopic measurements (see article and ESI 2.2) but not in general protein handling or apparent molecular mass on SDS-PAGE (see article and ESI 2.1). Both proteins crystallized in various conditions and yielded best diffracting crystals in different space groups, as described. To verify the intact assembly of monomers into the dodecameric hollow sphere, partly filled with dansyl, Cα-positions were examined.

A LSQ superposition (coot)[7, 8] was performed for both spheric dodecamers. The superposition of C_αs of chain A of dodecin_C59-dansyl on chain A of dodecin_wt resulted in negligible differences in the ribbon diagram for the rest of the correspondingly moved sphere (Fig. S12a).

A C_α-plot of all unique chains against chain A of dodecin_wt using the program superpose (CCP4i package)[3] showed low discrepancies for the three other chains within the asymmetric unit that can easily be explained by the imposed NCS-restraints (Fig: S12b). Remembering the different space group, the deviations for dodecin_C59-dansyl to chain A of dodecin_wt are little and give the normal, slightly increased scores at the

connections of secondary structure elements. Incorporation of modulators the size of dansyl with the additional feature of partly occupying the FMN binding pocket seem not disturb to the assembly of the intact quaternary structure of *M. tuberculosis* dodecin

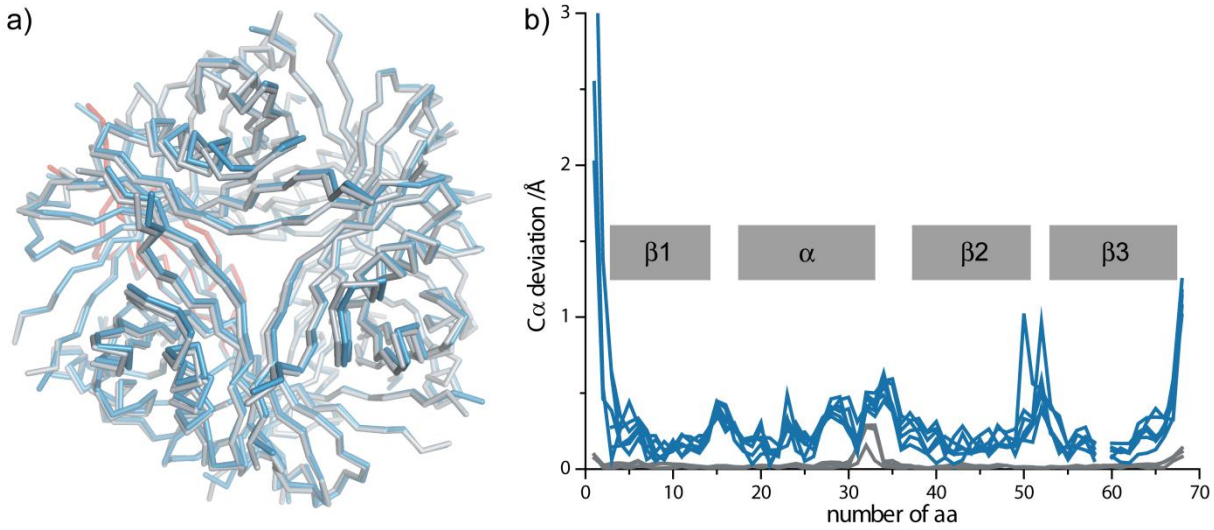

Fig. S12 Superposition of dodecin spheres. (a) Chain A of dodecin_C59-dansyl (grey) was superposed on reference chain A from dodecin_wt (red, background) whereas relative orientation of all other chains to chain A remained unchanged. (b) C_α-plot of all unique chains respective to chain A of dodecin_wt. The three chains of the wild type protein are given in grey, all six chains of dodecin_C59-dansyl are given in blue.

3. Abbreviations

aa - amino acid, amu – atomic mass units, CoA - Coenzyme A, CV - column volume, Da - Dalton, DTT – dithiothreitol, FMN - flavin mononucleotide, GdnCl - guanidinium chloride, IEX - ion exchange chromatography, MeCN - acetonitrile, MWCO - molecular weigth cut off, SEC - size exclusion chromatography, TCA - trichloroacetic acid, TCEP - Tris(2-carboxyethyl)phosphinehydrochloride

4. Literature

1. S. Reitz, M. Cebi, P. Reiss, G. Studnik, U. Linne, U. Koert and L.-O. Essen, *Angew. Chem.-Int. Ed.*, 2009, **48**, 4853-4857.
2. A. Leslie, *Joint CCP4+ ESF-EAMCB Newsletter on Protein Crystallography, Daresbury Laboratory Warrington*, 1992.
3. N. Collaborative Computational Project, *Acta Crystallogr., Sect. D: Biol. Crystallogr.*, 1994, **50**, 760-763.
4. A. Vagin and A. Teplyakov, *J. Appl. Crystallogr.*, 1997, **30**, 1022-1025.
5. B. Meissner, E. Schleicher, S. Weber and L.-O. Essen, *J. Biol. Chem.*, 2007, **282**, 33142-33154.
6. G. N. Murshudov, A. A. Vagin and E. J. Dodson, *Acta Crystallogr., Sect. D: Biol. Crystallogr.*, 1997, **53**, 240-255.
7. P. Emsley, B. Lohkamp, W. G. Scott and K. Cowtan, *Acta Crystallogr., Sect. D: Biol. Crystallogr.*, 2010, **66**, 486-501.
8. B. Lohkamp, P. Emsley and K. Cowtan, *CCP4 Newsletter*, 2005, **42**.
9. W. Kabsch, *J. Appl. Crystallogr.*, 1993, **26**, 795-800.
10. W. Kabsch, *Acta Crystallogr., Sect. D: Biol. Crystallogr.*, 2010, **66**, 125-132.
11. A. J. McCoy, R. W. Grosse-Kunstleve, P. D. Adams, M. D. Winn, L. C. Storoni and R. J. Read, *J. Appl. Crystallogr.*, 2007, **40**, 658-674.

12. W. Grosse, P. Reiß, S. Reitz, M. Cebi, W. Lübben, U. Koert and L.-O. Essen, *Bioorg. Med. Chem.*, 2010, **18**, 7716-7723.
13. B. K. Ho and F. Gruswitz, *BMC Struct. Biol.*, 2008, **8**, 49.
14. E. F. Pettersen, T. D. Goddard, C. C. Huang, G. S. Couch, D. M. Greenblatt, E. C. Meng and T. E. Ferrin, *J. Comput. Chem.*, 2004, **25**, 1605-1612.
15. K. A. Kantardjieff and B. Rupp, *Protein Sci.*, 2003, **12**, 1865-1871.
16. H. Chosrowjan, S. Taniguchi, N. Mataga, F. Tanaka, D. Todoroki and M. Kitamura, *J. Phys. Chem. B*, 2007, **111**, 8695-8697.
17. H. Du, R. A. Fuh, J. Li, A. Corkan, J. S. Lindsey, *Photochem. Photobiol.*, 1998, **68**, 141-142.
18. E. Gasteiger, C. Hoogland, A. Gattiker, S. Duvaud, M.R. Wilkins, R.D. Appel, A. Bairoch in *The Proteomics Protocols Handbook*, ed. J.M. Walker, Humana Press, 2005, 571-607.